JACS
JOURNAL OF THE AMERICAN CHEMICAL SOCIETY

COMMUNICATION

pubs.acs.org/JACS

Mixed-Metal Pt Monolayer Electrocatalysts with Improved CO Tolerance

Anand Udaykumar Nilekar,[§,†,‡] Kotaro Sasaki,[⊥,‡] Carrie A. Farberow,[§] Radoslav R. Adzic,[⊥] and Manos Mavrikakis*[,§]

[§]Department of Chemical & Biological Engineering, University of Wisconsin—Madison, Madison, Wisconsin 53706, United States
[⊥]Chemistry Department, Building 555, Brookhaven National Laboratory, Upton, New York 11973, United States

Supporting Information

ABSTRACT: Using a combination of periodic, self-consistent, density functional theory (DFT) calculations and CO-stripping voltammetry experiments, we have designed a new class of Pt−M bimetallic monolayer catalysts supported on a non-Pt metal, which exhibit improved stability against CO poisoning and might be suitable for proton-exchange membrane fuel cell anodes. These surfaces help in reducing the overpotential associated with anodic CO oxidation and minimize the amount of Pt used, thereby reducing materials cost. DFT calculations predict highly repulsive interactions between adsorbed CO molecules on these surfaces, leading to weaker binding and lower coverage of CO than on pure Pt, which in turn facilitates oxidative removal of CO from these catalytic surfaces.

Platinum, the monometallic catalyst of choice for the anode of low-temperature fuel cells (FCs), shows very high activity for the electro-oxidation of pure hydrogen. However, even trace amounts of carbon monoxide present in the reformate H_2/CO mixture tend to poison the catalyst surface and substantially increase the overpotential for this reaction (~0.7 V).[1,2] As a result, identifying a CO-tolerant catalyst with low Pt content has been the primary interest of several experimental[3−6] and theoretical[7,8] studies. Various Pt alloys (e.g., PtRu, PtMo, PtSn) have been proposed and shown to have high CO tolerance, leading to lower overpotentials because of ligand effects and the bifunctional nature of the catalyst.[9] In this Communication, by using a combination of density functional theory (DFT) calculations and electrocatalytic experiments, we demonstrate an informed approach to designing a new class of anode alloy electrocatalysts with lower Pt content and improved CO tolerance.

In an earlier study focused on the oxygen reduction reaction (ORR) occurring at the cathode side of FCs, we showed that, by depositing a single Pt monolayer on other metal substrates, the reactivity of platinum atoms can be manipulated by exploiting the strain and ligand effects.[10] Furthermore, the replacement of a fraction of the Pt overlayer atoms with atoms of a more oxophillic metal yielded remarkable improvements in ORR rates,[11] mainly by destabilizing OH intermediates on the Pt sites of the catalytic surface. Inspired by the enhanced performance of these ternary alloy cathode catalysts, we present here the design of an analogous class of anode electrocatalysts. By suitable choice of the support metal and the metal to be mixed with Pt atoms in the overlayer, highly active electrocatalysts for the anodic H_2 electro-oxidation in the presence of CO are designed from first principles, prepared in a single-crystal form, and characterized for electrocatalytic activity experimentally. The repulsive interaction between CO molecules on the alloy surface is identified as a key reactivity descriptor.

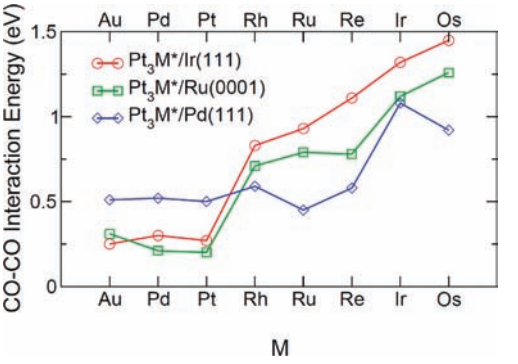

Figure 1. Absolute CO−CO interaction energy [BE(θ_{CO} = $^1/_2$ ML) − 2BE(θ_{CO} = $^1/_4$ ML)] on various model surfaces. Positive interaction energies indicate repulsive co-adsorption.

First, using DFT calculations, we evaluate the combined strain and ligand effects of depositing a Pt monolayer on Ir(111), Ru(0001), and Pd(111) surfaces (see Supporting Information (SI) for details of the calculations). CO binding energies at $^1/_4$ ML coverage on these surfaces are −1.27, −1.25, and −1.87 eV, respectively. Compared to a value of −1.82 eV on pure Pt(111), Pt*/Ir(111) and Pt*/Ru(0001) show significant reduction in CO binding energy, because of the compressive strain within the Pt overlayer, induced by the smaller lattice constant of the supporting metal, and the ligand effect between Pt and the support metal. Next, we replace $^1/_4$ ML of the surface Pt atoms with another metal (M), yielding surface compositions of Pt_3M for the overlayer. Subsequently, and in order to evaluate the CO−CO interaction energetics, the CO binding energies at coverages of $^1/_4$ and $^1/_2$ ML are calculated. Figure 1 shows the CO−CO interaction energies for all Pt_3M overlayers on Ir(111), Ru(0001), and Pd(111). Figure S2 (SI) shows the calculated most stable configurations for CO at $^1/_2$ ML coverage on Pt_3M overlayers on Ir(111), which yields the most promising ternary alloy compositions from those investigated here (see Figure 1).

The CO−CO interaction energies are positive for all M's considered in this study, indicating repulsive interactions,

Received: August 4, 2011
Published: October 25, 2011

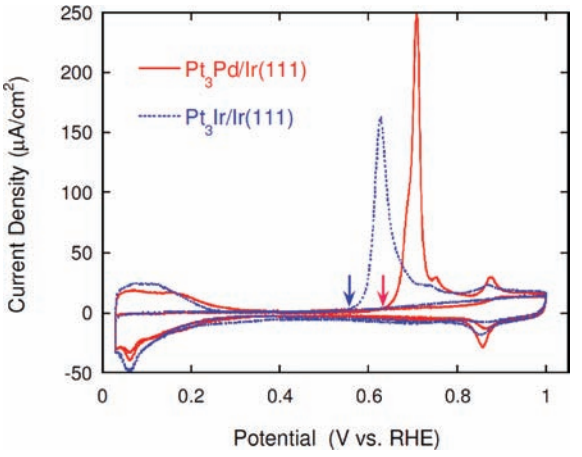

Figure 2. CO-stripping peaks from the $Pt_3Pd^*/Ir(111)$ and $Pt_3Ir^*/Ir(111)$ surfaces, obtained by sweeping the potential at a rate of 20 mV/s in 0.1 M $HClO_4$ purged by Ar. CO adsorption on the surfaces was done by holding the electrode in a $HClO_4$ solution at a constant potential of 0.23 V while CO was introduced into the cell. The blue and red arrows indicate the onset potential for CO oxidation on the $Pt_3Ir^*/Ir(111)$ and $Pt_3Pd^*/Ir(111)$ surfaces, respectively.

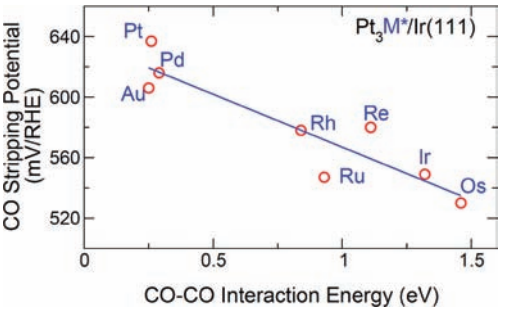

Figure 3. Measured CO-stripping potential on various $Pt_3M^*/Ir(111)$ surfaces as a function of the calculated absolute CO−CO repulsion energy in a 2×2 unit cell. The blue line is the best-fit line for the Ir(111)-supported Pt_3M monolayer systems: [CO-stripping potential (mV/RHE)] = 636.8 − 69.8 × [CO−CO interaction energy (eV)]; $R^2 = 0.84$.

destabilizing CO as its surface coverage increases. On $Pt_3M^*/Ir(111)$ surfaces, repulsion between CO molecules increases in the order M = Au, Pd, Pt < Rh < Ru < Re < Ir < Os. The higher the CO−CO repulsion energy, the more CO-tolerant the surface should be. For example, in the case of $Pt_3Os^*/Ir(111)$, the repulsion energy is 1.45 eV. At $^1/_4$ ML CO coverage, the binding energies for the first CO on $Pt^*/Ir(111)$ and $Pt_3Os^*/Ir(111)$ surfaces are −1.27 and −2.29 eV, respectively. At $^1/_2$ ML CO coverage, however, the differential binding energy for the second CO on the $Pt_3Os^*/Ir(111)$ is −0.83 eV, which is considerably lower compared to the respective differential binding energy of −1.01 eV on the $Pt^*/Ir(111)$ surface. For the model surfaces studied here, and for cases with high CO−CO repulsion energies, the first CO molecule ($\theta_{CO} = {}^1/_4$ ML) adsorbing in this unit cell goes onto highly reactive M atoms, whereas the second CO molecule ($\theta_{CO} = {}^1/_2$ ML) adsorbs on sites defined by Pt atoms only. The CO−CO interaction energies on the $Pt_3M^*/Ru(0001)$ and $Pt_3M^*/Pd(111)$ surfaces follow trends similar to those found for $Pt_3M^*/Ir(111)$, with some variations because of different strain and ligand effects.

Because H_2 electro-oxidation in itself is a relatively facile reaction on the Pt(111) surface, the overpotential for that reaction originates from the CO poisoning of that surface.[12] Watanabe[9] has proposed that the main reactivity descriptor for Pt-based anode catalysts is their CO binding characteristics. Higher CO−CO repulsion energy is expected to favor weaker Pt−CO interaction and lead to lower CO coverages. Therefore, we expect that Pt_3M overlayers on different substrate metals, characterized by high CO−CO repulsion energies, will show high reactivity toward H_2 electro-oxidation in the presence of CO.

Given the above theoretical findings, we focused our experimental efforts on systems with Ir(111) as the support of the Pt_3M overlayer. Accordingly, we synthesized electrocatalysts comprising a Pt_3M monolayer (M = Au, Pt, Pd, Ir, Rh, Re, or Os) on an Ir(111) surface and then performed oxidative CO desorption experiments on these model surfaces. As an example, the voltammetry curves for the deposition of a single Pt_3Rh overlayer on the Ir(111) single-crystal surface are shown in Figure S3 (SI).

CO adsorption on the resultant $Pt_3M^*/Ir(111)$ surfaces is performed by holding the electrode in a $HClO_4$ solution at a constant potential of 0.23 V (at which no CO oxidation takes place on the surface) while CO is introduced into the cell. CO is then removed from the solution through purging by Ar in order to study its anodic stripping from the surface. Figure 2 presents the oxidative CO desorption from Pt_3Pd ML and Pt_3Ir ML, each supported on Ir(111), by sweeping the potential from 30 mV. Figure 2 shows that CO adlayers on the surfaces exhibit completely suppressed peaks in the hydrogen adsorption/desorption region. The onset of CO oxidation occurs at a less positive potential on the $Pt_3Ir^*/Ir(111)$ surface (0.55 V) than on the $Pt_3Pd^*/Ir(111)$ surface (0.62 V), both lower than that on a pure Pt(111) surface (∼0.70 V),[1] indicating a significant effect of the addition of metal M on the bonding of CO to Pt and also the enhanced CO−CO repulsion.

Further, we compare the theoretically calculated CO−CO repulsion energy with the experimentally observed CO-stripping potential on the $Pt_3M^*/Ir(111)$ surfaces. As shown in Figure 3, there is a good linear correlation between these two quantities, which rationalizes our underlying design hypothesis that CO destabilization, as controlled by surface composition, is a key factor determining eletrocatalytic activity. In particular, the CO-stripping potential drops from ∼0.7 V on pure Pt(111) to 0.64 V for $Pt^*/Ir(111)$, because of weaker Pt−CO binding due to the compressive strain imparted by the Ir(111) substrate on the Pt overlayer. Further, an additional ∼100 mV decrease in the CO-stripping potential is realized by going from $Pt^*/Ir(111)$ to $Pt_3Ir^*/Ir(111)$ or $Pt_3Os^*/Ir(111)$. This additional improvement originates from the increased repulsive interaction between CO molecules on the bimetallic Pt_3M overlayer.

To elucidate the importance of the metal substrate, we then calculated the CO binding energy (for $^1/_4$ and $^1/_2$ ML coverages) on the (111) facet of the Pt_3Ir bulk alloy, which exposes a monolayer of Pt_3Ir on the surface, identical to the overlayer in the $Pt_3Ir^*/Ir(111)$ system, but in the case of Pt_3Ir bulk alloy that monolayer is supported by Pt_3Ir, not Ir(111). On this Pt_3Ir bulk alloy, the first CO ($^1/_4$ ML) binds to the (111) surface with a binding energy of −2.35 eV, whereas on $Pt_3Ir^*/Ir(111)$ this value is −2.16 eV. The differential binding energy of the second CO ($^1/_2$ ML) on the (111) facet of Pt_3Ir is −1.37 eV, and the repulsion energy is 0.98 eV. The respective values on $Pt_3Ir^*/Ir(111)$ are −0.85 and 1.32 eV. Therefore, the (111) terminated bulk alloy clearly binds CO more strongly than $Pt_3Ir^*/Ir(111)$ at all coverages probed and exhibits weaker CO−CO repulsion

than $Pt_3Ir^*/Ir(111)$. As a result, the (111) facet of Pt_3Ir bulk alloy is expected to have inferior CO tolerance compared to the $Pt_3Ir^*/Ir(111)$ overlayer structure. Our findings suggest that the improved CO tolerance recently reported for PtIr bimetallic alloys in electro-oxidation reactions[13] may have been the consequence of adsorbate-induced segregation, leading to the in situ formation of Ir-rich subsurface layers, effectively resembling the more CO-tolerant $Pt_3Ir^*/Ir(111)$ structure identified in our studies.

Finally, we briefly comment on two relevant issues: (i) Under typical reaction conditions, anode catalysts are expected to be partially covered by OH species. Our studies do not account for the co-adsorption of OH with CO, which could lead to the bifunctional mechanism for CO electro-oxidation. Further studies would be needed to address possible interactions between these two adsorbed species. Yet, the results shown in Figure 3 strongly suggest that the CO−CO interaction is a key reactivity descriptor, even if not the only one. (ii) Analogous overlayer structures studied in the context of ORR electrocatalysis were remarkably stable, some of them more stable than Pt, due to their increased resistance of oxidation. Nevertheless, the long-term stability of the mixed-metal Pt monolayer supported on other metals, such as Ir and Ru, under anodic electro-oxidation conditions needs to be investigated separately.

In conclusion, using first-principles calculations, we have screened a number of mixed-metal Pt monolayer compositions supported on other metals and identified a small set of promising CO-tolerant Pt−M mixed monolayers supported on Ir(111). Experimentally, these alloys showed high reactivity and lower overpotential for CO-stripping compared to pure Pt(111). The CO-stripping overpotential decreases with increasing CO−CO repulsion energy. These electrocatalysts present attractive alternatives to existing catalysts as a result of their decreased cost, high Pt mass-specific activity, enhanced CO tolerance, and resultant reduction in overpotential for electro-oxidation of H_2 in the presence of CO. The molecular-level understanding provided by DFT calculations suggests that the enhanced CO tolerance originates from an increased repulsive interaction between adsorbed CO molecules, mediated by the novel electronic structure of these bimetallic monolayer surfaces, which are supported by a non-Pt metal.

■ ASSOCIATED CONTENT

Supporting Information. Theoretical and experimental methods and binding energies for various alloys. This material is available free of charge via the Internet at http://pubs.acs.org.

■ AUTHOR INFORMATION

Corresponding Author
manos@engr.wisc.edu

Present Addresses
[†]Shell Oil Co., Westhollow Technology Center, Houston, TX 77082

Author Contributions
[‡]These authors contributed equally.

■ ACKNOWLEDGMENT

This work is financially supported by DOE-BES, Chemical Sciences Office, under contract no. DE-FG02-05ER15731. C.A.F. thanks NSF for a Graduate Research Fellowship under Grant No. DGE-0946806. Calculations were performed by using supercomputing resources at: EMSL, a national scientific user facility located at Pacific Northwest National Laboratory; the National Center for Computational Sciences (NCCS) at Oak Ridge National Laboratory; and the National Energy Research Scientific Computing Center (NERSC). EMSL is sponsored by the US Department of Energy's Office of Biological and Environmental Research. NCCS and NERSC are supported by the Office of Science of the US Department of Energy under Contract No. DE-AC05-00OR22725 and DE-AC02-05CH11231, respectively.

■ REFERENCES

(1) Gottesfeld, S.; Zawodzinski, T. A. *Advances in Electrochemical Science and Engineering*; Wiley VCH: Weinheim, Germany, 1997; Vol. 5.
(2) Markovic, N. M. *Handbook of Fuel Cells—Fundamentals, Technology and Applications*; Wiley: Hoboken, NJ, 2003; Vol. 2, 368−393.
(3) Brankovic, S. R.; Wang, J. X.; Adzic, R. R. *Electrochem. Solid State Lett.* **2001**, *4*, A217.
(4) Gasteiger, H. A.; Markovic, N. M.; Ross, P. N. *J. Phys. Chem.* **1995**, *99*, 8290.
(5) Gasteiger, H. A.; Markovic, N. M.; Ross, P. N. *J. Phys. Chem.* **1995**, *99*, 16757.
(6) Mukerjee, S.; Lee, S. J.; Ticianelli, E. A.; McBreen, J.; Grgur, B. N.; Markovic, N. M.; Ross, P. N.; Giallombardo, J. R.; De Castro, E. S. *Electrochem. Solid State Lett.* **1999**, *2*, 12.
(7) Liu, P.; Logadottir, A.; Nørskov, J. K. *Electrochim. Acta* **2003**, *48*, 3731.
(8) Davies, J. C.; Bonde, J.; Logadottir, A.; Nørskov, J. K.; Chorkendorff, I. *Fuel Cells* **2005**, *5*, 429.
(9) Watanabe, M. *Handbook of Fuel Cells—Fundamentals, Technology and Applications*; Wiley: Hoboken, NJ, 2003; Vol. 2, 408−415.
(10) Zhang, J. L.; Vukmirovic, M. B.; Xu, Y.; Mavrikakis, M.; Adzic, R. R. *Angew. Chem., Int. Ed.* **2005**, *44*, 2132.
(11) Zhang, J. L.; Vukmirovic, M. B.; Sasaki, K.; Nilekar, A. U.; Mavrikakis, M.; Adzic, R. R. *J. Am. Chem. Soc.* **2005**, *127*, 12480.
(12) Nilekar, A. U.; Alayoglu, S.; Eichhorn, B.; Mavrikakis, M. *J. Am. Chem. Soc.* **2010**, *132*, 7418.
(13) Kim, S. K.; Hwang, S. J.; Yoo, S. J.; Jeon, T. Y.; Lee, K. S.; Lim, T. H.; Sung, Y. E. *Chem. Commun.* **2010**, *46*, 8401.